HHS Public Access

Author manuscript

IEEE Trans Appl Supercond. Author manuscript; available in PMC 2018 June 01.

Published in final edited form as:

IEEE Trans Appl Supercond. 2017 June ; 27(4): . doi:10.1109/TASC.2016.2633626.

Test of an 8.66-T REBCO Insert Coil with Overbanding Radial Build for a 1.3-GHz LTS/HTS NMR Magnet

Timing Qu,
Francis Bitter Magnet Laboratory, Plasma Science and Fusion Center, M.I.T., Cambridge MA, U.S.A. Department of Mechanical Engineering, and State Key Laboratory of Tribology, Tsinghua University, China. He participated in this work while a visiting scientist at MIT, March 2015-February 2016

Philip C. Michael,
Francis Bitter Magnet Laboratory, Plasma Science and Fusion Center, M.I.T., Cambridge MA, U.S.A

Juan Bascuñán,
Francis Bitter Magnet Laboratory, Plasma Science and Fusion Center, M.I.T., Cambridge MA, U.S.A

Thibault Lécrevisse,
Francis Bitter Magnet Laboratory, Plasma Science and Fusion Center, M.I.T., Cambridge MA, U.S.A

Mingzhi Guan,
Francis Bitter Magnet Laboratory, Plasma Science and Fusion Center, M.I.T., Cambridge MA, U.S.A

Seungyong Hahn, and
National High Magnetic Field Laboratory and Florida State University, Tallahassee FL, U.S.A

Yukikazu Iwasa
Francis Bitter Magnet Laboratory, Plasma Science and Fusion Center, M.I.T., Cambridge MA, U.S.A

Abstract

A 1.3-GHz/54-mm LTS/HTS NMR magnet, assembled with a 3-coil (Coils 1–3) 800-MHz HTS insert in a 500-MHz LTS NMR magnet, is under construction. The innermost HTS insert Coil 1 has a stack of 26 no-insulation (NI) double pancake (DP) coils wound of 6-mm wide and 75-μm thick REBCO tapes. In order to keep the hoop strains on REBCO tape < 0.6% at an operating current I_{op} of 250 A and in a field of 30.5 T, we overbanded each pancake in Coil 1 with a 6-mm wide, 76-μm thick 304 stainless steel strip: 7-mm thick radial build for the central 18 pancakes, while 6-mm thick for the outer 2×17 pancakes. In this paper, Coil 1 was successfully tested at 77K and 4.2 K. In the 77-K test, the measured critical current was 35.7 A, determined by an *E*-field criterion of 0.1 μV/cm. The center field magnet constant decreased from 34.2 mT/A to 29.3 mT/A,

Correspondence to: Timing Qu.

when I_{op} increased from 5 A to 40 A. The field distribution at different I_{op} along the z-axis was measured. The residual field distributions discharged from 10 A and 20 A were recorded. In the 4.2-K test, Coil 1 successfully generated a central field of 8.78 T at 255 A. The magnet constant is 34.4 mT/A, which is same as our designed value. The field homogeneity at the coil center within a ±15-mm region is around 1700 ppm. This large error field must be reduced before field shimming is applied.

Index Terms

NMR magnet; no-insulation; double pancake; overbanding

I. Introduction

High temperature superconducting (HTS) technology is considered to be one major solution for the NMR magnet above 1 GHz. In NMR, high magnetic field leads to improved resolution and higher sensitivity, which enables the efficient and sensitive examination of complex molecular systems. A high resolution 1.3-GHz NMR magnet (1.3G) is now under development in the Francis Bitter Magnet Laboratory, Plasma Science and Fusion Center at MIT. This magnet is composed of a 500-MHz low-temperature (LTS) NMR magnet and an 800-MHz HTS one (H800) including three nested HTS coils (Coils 1, 2, 3) [1]–[3]. The combination of an LTS magnet with HTS insert was proved to be an effective way to achieve high fields above 20 T [4]–[9]. Clearly the center field in the 1.3G has a greater contribution (18.78 T) from the HTS insert, than the 11.74 T from the LTS magnet.

H800 requires high current density considering the limited installing space inside L500. No-insulation (NI) winding technique [10]–[15] is applied to all double pancakes (DP) in H800. NI coils were proved to be self-protected [16]–[18], mechanical integrity, and compactness [2], which enables a high critical current density in HTS turns to generate high magnetic field. H800 operated in the 30.5 T background also requires high mechanical strength. The calculation [1] shows that H800 should not only be split to three nested coils, but also be overbanded to reduce the hoop strain below 0.6% [2], [12], [19].

We reported our recent progress on the 1.3G project in this paper. The innermost Coil 1 was fully-overbanded and tested at 77 K and 4.2 K. The $V(I)$ characteristics and the center field magnet constant were measured. The screening-current-induced residual field at 77 K was measured. The axial field distributions at different I_{op} were also mapped and discussed.

II. Overbanding for Coil 1

H800 is a combination of three nested HTS coils. Coil 1, the innermost, has been fully constructed and tested. As shown in Fig. 1, Coil 1 was assembled by 26 DP coils, wound of 6-mm wide and 75-μm thick REBCO tape produced by SuperPower. 5-mil G10 spacers were placed between pancakes. Central 6 DPs were inside-notched to improve the field homogeneity. Adjacent DPs were lap jointed through 12-mm wide REBCO splices [3]. Stress analysis shows that the hoop stress when fully energized will exceed the strength limit of REBCO tapes, even that H800 has been separated into three nested coils [1], [20]. Each

single pancake coil should be overbanded with strong metallic tapes of high Young's modulus and yielding stress. It was calculated that a 6-mm thick overbanding radial build, wound by a 76-μm thick stainless steel (SS) tape with a 50-N winding tension, would reduce the hoop stress in Coil 1 below 700 MPa [20]. In this work, we choose overband thickness of 6 mm for the top 17 and bottom 17 pancakes, and 7-mm thick for the central 18 pancakes. This is because the central 18 pancakes, exposed to higher magnetic fields than those in top and bottom halves, must withstand larger hoop stresses.

We first built a 21-layer (roughly 1.6-mm thick) overband for each pancake to test the winding technique. Then Coil 1 was fully overbanded to the target thickness with the same SS tape and winding parameters (see Fig. 2). The properties and key parameters of the fully-overbanded Coil 1 are listed in Table I. Coil 1 was then tested at 77 K in liquid nitrogen and 4.2 K in liquid helium, to verify if any of the splices or tapes have been damaged during the overbanding process.

III. Test of Coil 1 at 77 K in liquid nitrogen

Coil 1, placed in a bath of liquid nitrogen, was operated in series of a charge-hold-discharge (i.e., a trapezoidal) time function with charge and discharge rates respectively at ±2 A/min. The hold-current level, each lasting ~60 min, was increased in a 5-A increment up to 25 A, and then in smaller increments up to 40 A. Voltage taps, soldered to the top and bottom pancakes, respectively, the 52th and 1st, measured the global voltage signal. To reach a stable current distribution in this NI Coil 1, we hold the current at each step for > 10 τ, the time constant calculated by L_m/R_m, where L_m is the Coil 1 inductance and R_m is the radial resistance determined by the equivalent circuit model [10], [11]. With a Hall probe the axial field distribution was mapped at selected currents. After discharging Coil 1 from 10 A and 20 A, we measured the axial screening-current-induced residual field.

Fig. 3 shows typical voltage and field evolution curves during the charging process of Coil 1. The voltage increased fast during current ramping and then dropped exponentially to zero, a result of the current redistribution within NI turns when the current was held. The equivalent circuit model is also applicable for Coil 1. We may ignore the ac loss dissipation in HTS DPs and intra pancake joint ($25R_j$) dissipation, both of which are much smaller than R_m dissipation. The left side of the voltage curve (increasing part) in Fig. 3 can be fit by

$$V_c(t)=\alpha L_m(1-e^{-t/\tau}), \quad (1)$$

where α = 0.033 A/s. The right side of the voltage curve (decreasing part) is a typical exponential decay determined by the time constant τ. By fitting the left side and the decay part of each voltage curves, we may determine, respectively, L_m and τ, and thus $R_m = L_m/\tau$. Calculated values for L_m, τ and R_m are shown in Table II. L_m is slightly smaller than the designed value (2.43 H), but still in the acceptable range. τ and R_m are nearly current-independent in the 10–25 A range.

The stable coil voltage measured after a long hold time is shown in Fig. 4. The critical current, I_c, is 35.7 A under a criterion of 0.1 μV/cm, which is the same as before overbanding. A resistive voltage appeared above 25 A. Pancakes #4, #6 and #11, show clear resistive voltage signals when charged above 20A. The equivalent coil resistance R_{ec} calculated from the $V(I)$ curves increased from 3.2 $\mu\Omega$ at 10 A to 24.9 $\mu\Omega$ at 25 A and 1.61 mΩ at 40 A. This nonlinear R_{ec} comes from a combination of the joint resistance of 51 splices, flux flow resistance in HTS loops, and R_m as well.

The center field (B_0) magnet constant calculated by B_0/I_{op} dropped from 34.2 mT/A at 10 A to 29.3 mT/A at 40 A, with a sharp turning at 25 A. Because of R_{ec}, a small current will bypass through R_m, which does not contribute to the center field, therefore suppresses the magnet constant. The calculated magnet constant according to the circuit model is also shown Fig. 4. There are discrepancies between the measurement and calculation at large I_{op}. The flux flow resistance of each pancake is determined by the critical current, which is both field-dependent and angular-dependent. Thus the bypass current in different pancakes may not be uniform, since the field varies within Coil 1. Our circuit model [10], [11] does not consider this phenomenon. Clearly, it needs to be more comprehensive to include these sublet but important issues.

Using a Hall sensor, we measured the axial field distribution of Coil 1. The field plots normalized to the center field (B_0) are shown in Fig. 5. The field homogeneity inside a ±15-mm region is < 1500 ppm for I_{op} ≤25 A. We believe that the screen current (SC) field contributes a lot to the asymmetry field distribution. Errors related to the number of turns and coil dimensions may also be important reasons for the field inhomogeneity. It is clear that the shape of the curves changes with increasing I_{op}, which is a typical behavior of NI coils. As discussed above, the actual superconducting current path within each HTS pancake differs from pancake to pancake, as determined by each pancake's electromagnetic and mechanical properties and the field it is exposed to. This non-uniform current in different pancakes certainly influences the shape of field distribution patterns. When I_{op} > 25A, some pancakes, such as #4, #6 and #11, show an obviously resistive behavior. The spiral current flowing inside these pancakes will be reduced and the field homogeneity of Coil 1 degraded.

Fig. 6 shows the axial residual field plots after the coil was discharged from 10A and 20A. This small residual field comes from the SC field induced by the self field of the magnet [21], [22]. The amplitude of the SC field at the coil center is about 1.3% of the original center field, which is huge. However, the error field introduced by the SC field within the ±15-mm region is around several hundred ppm, which may be reduced by the "field-shaking" technique [2], [23]. The temporal behavior of the SC field is also a big issue, which strongly depends on the excitation history [24].

IV. Test of Coil 1 at 4.2 K in liquid helium

After the 77-K test, the overbanded Coil 1 was also tested at 4.2 K in liquid helium. There were two test sequences, as shown in Fig. 7. The first sequence has two current plateaus at 100 A and 220 A. The second one has one plateau of 255 A, ~ 4 A larger than the rated I_{op} = 251.3 A of our 1.3G. The current ramp rate was 5A/min. We held current for over 70min at

each current plateau for stabilizing. The voltage vs. time curve is also drawn in Fig. 7. As for the 77-K test, We can fit the the voltage curve to determine L_m, τ and R_m from (1) and the exponential decay function. The results are shown in Table III. L_m is quite close to the designed value (2.43 H), which means that Coil 1 works well and did not loose any turns during the 4.2-K operation. R_m is much smaller than the 77-K value (9.7 mΩ). Apart from the lower temperature, the stronger magnetic field may produce a better turn-to-turn contact. Both factors may lead to a smaller R_m.

Normalized axial field (B/B_0) distribution along the axis of Coil 1 is shown in Fig. 8. Within our measurement range and resolution, the distribution patterns look quite similar to each other. The curve for the case of 10 A at 77 K is also drawn in Fig. 8, which approximately agrees with the 4.2-K result. Coil 1 generated 8.78 T at 255 A, exceeding our target value of 8.66 T. The magnet constant calculated by B_0/I_{op} is quite close to the designed value. This result confirms that the 255-A stand-alone operation of Coil 1 was safe and successful. There are no signs of abnormality or bypass current through R_m. For the case of 255-A operation, the field homogeneity inside a ±15-mm region is ~ 1700 ppm. This large error field must be reduced by the shaking-field technique before field shimming is applied.

V. Conclusion

The innermost HTS insert coil (Coil 1) for a 1.3-GHz LTS/HTS NMR magnet was successfully built and tested. Coil 1 was constructed by 26 double pancakes wound with 6-mm wide and 75-μm thick REBCO HTS tapes by using no-insulation technique. Each pancake was overbanded by a 76-μm thick stainless steel tape in order to reduce the hoop strain below 0.6% when operated in the 1.3 GHz condition. In the 77-K test, the I_c of Coil 1 is 35.7 A under the criterion of 0.1 μV/cm. The magnet constant, center field (B_0) divided by the operation current (I_{op}), kept around 34.2 mT/A until I_{op} = 25 A, then dropped to 29.3 mT at I_{op} = 40 A, which can be explained by the bypass current through the contact resistance of the NI Coil 1. After discharging Coil 1 from 10 A and 20 A, a residual field clearly appeared, which comes from the screening current (SC) field. The amplitude of this SC field in the center position is ~1.3% of the original field. In the 4.2-K test, Coil 1 was successfully charged up to B_0 = 8.78 T at I_{op} = 255 A. The magnet constant is 34.4 mT/A, the same as our designed value. The field homogeneity at the coil center in a ±15-mm region is ~ 1700 ppm, which must be reduced before shimming.

Acknowledgments

This work was supported by the National Institute of General Medical Sciences (Grant 9R01GM114834-11) of the National Institutes of Health. Timing Qu was partly supported by the National Natural Science Foundation of China (Grant 51475257) and the State Scholarship Fund of China.

References

1. Bascuñán J, Hahn S, Kim Y, Song J, Iwasa Y. 90-mm/18.8-T all HTS insert magnet for 1.3 GHz LTS/HTS NMR application: Magnet design and double pancake fabrication. IEEE Trans Appl Supercond. Jun.2014 24(3) Art. no. 4300904.

2. Bascuñán J, Hahn S, Lécrevisse T, Song J, Miyagi D, Iwasa Y. An 800-MHz all-REBCO insert for the 1.3-GHz LTS/HTS NMR magnet program - a progress report. IEEE Trans Appl Supercond. Jun. 2016 26(4) Art. no. 4300205.
3. Lécrevisse T, Bascuñán J, Hahn S, Kim Y, Song J, Iwasa Y. Pancake-pancake joint resistances of a magnet assembled from GdBCO double-pancake coils. IEEE Trans Appl Supercond. Jun.2016 25 Art. no. 6602505.
4. Wang Q-L, et al. High magnetic field superconducting magnet system up to 25 T for ExCE. IEEE Trans Appl Supercond. 2013; 23 Art. no. 4300905.
5. Wang Q-L, et al. High temperature superconducting YBCO insert for 25 T full superconducting magnet. IEEE Trans Appl Supercond. Jun.2015 25(3) Art. no. 4603505.
6. Liu J-H, Song S-S, Wang Q-L, Zhang Q-J. Critical current analysis of an YBCO insert for ultrahigh-field all-superconducting magnet. IEEE Trans Appl Supercond. 2016; 26(3) Art. no. 4303405.
7. Awaji S, et al. New 25 T cryogen-free superconducting magnet project at Tohoku University. IEEE Trans Appl Supercond. 2014; 24(3) Art. no. 4302005.
8. Koyanagi K, et al. Design of a 30 T superconducting magnet using a coated conductor insert. IEEE Trans Appl Supercond. 2009; 19(3):1617–1620.
9. Trociewitz UP, et al. 35.4 T field generated using a layer-wound superconducting coil made of (RE)$Ba_2Cu_3O_{7-x}$ (RE=rare earth) coated conductor. Appl Phys Lett. 2011; 99(20) Art. no. 222506.
10. Hahn S, Park DK, Bascuñán J, Iwasa Y. HTS pancake coils without turn-to-turn insulation. IEEE Trans Appl Supercond. Jun; 2011 21(3):1592–1595.
11. Wang X, et al. Turn-to-turn contact characteristics for an equivalent circuit model of no-insulation Re[RE]BCO pancake. Supercond Sci Technol. 2013; 26 Art. no. 035012.
12. Hahn S, Park DK, Voccio J, Bascuñán J, Iwasa Y. No-insulation (NI) HTS inserts for >1GHz LTS/HTS NMR magnets. IEEE Trans Appl Supercond. 2012; 22 Art. no. 4302405.
13. Hahn S, et al. No-insulation coil under time-varying conditions: charging delay and magnetic coupling. Supercond Sci Technol. 2013; 23 Art. no. 4601705.
14. Hahn S, et al. No-insulation multi-width winding technique for high temperature superconducting magnet. Appl Phys Lett. 2013; 103 Art. no. 173511.
15. Wang Y, Song H. Influence of turn-to-turn resistivity and coil geometrical size on charging characteristics of no-electrical-insulation REBCO pancake coils. Supercond Sci Technol. 2016; 29 Art. no. 075006.
16. Kim YG, Hahn S, Kim KL, Kwon OJ, Lee H. Investigation of HTS racetrack coil without turn-to-turn insulation for superconducting rotating machines. IEEE Trans Appl Supercond. Jun.2012 22(3) Art. no. 5200604.
17. Kim K, et al. Operating characteristics of an insulationless HTS magnet under the conduction cooling condition. IEEE Trans Appl Supercond. Jun.2013 23(3) Art. no. 4601504.
18. Wang Y, et al. An equivalent circuit grid model for no-insulation HTS pancake coils. Supercond Sci Technol. Mar.2015 28(4) Art. no. 045017.
19. Nakasaki, R., et al. Technology and Manufacturing Innovations at SuperPower. 2015. [Online]. Available: http://www.superpower-inc.com/content/technical-documents
20. Guan M, et al. A parametric study on overband radial build for a REBCO 800-MHz insert of a 1.3-GHz LTS/HTS NMR magnet. IEEE Trans Appl Supercond. Jun.2016 26(4) Art. no. 4301205.
21. Gu C, Qu T, Han Z. Measurement and calculation of residual magnetic field in a Bi2223/Ag Magnet. IEEE Trans Appl Supercond. 2007; 17:2394–2397.
22. Hahn S, Bascuñán J, Kim W-S, Bobrov ES, Lee H, Iwasa Y. Field Mapping, NMR lineshape, and screening currents induced field analyses for homogeneity improvement in LTS/HTS NMR magnets. IEEE Trans Appl Supercond. 2008; 18:856–859.
23. Kajikawa K, Gettliffe GV, Chu Y, Miyagi D. Designs and tests of shaking coils to reduce screening currents induced in HTS insert coils for NMR magnet. IEEE Trans Appl Supercond. 2015; 25(3): 1–5.
24. Amemiya N, et al. Temporal behaviour of multi-pole components of the magnetic field in a small dipole magnet wound with coated conductors. Supercond Sci Technol. 2015; 28 Art. no. 035003.

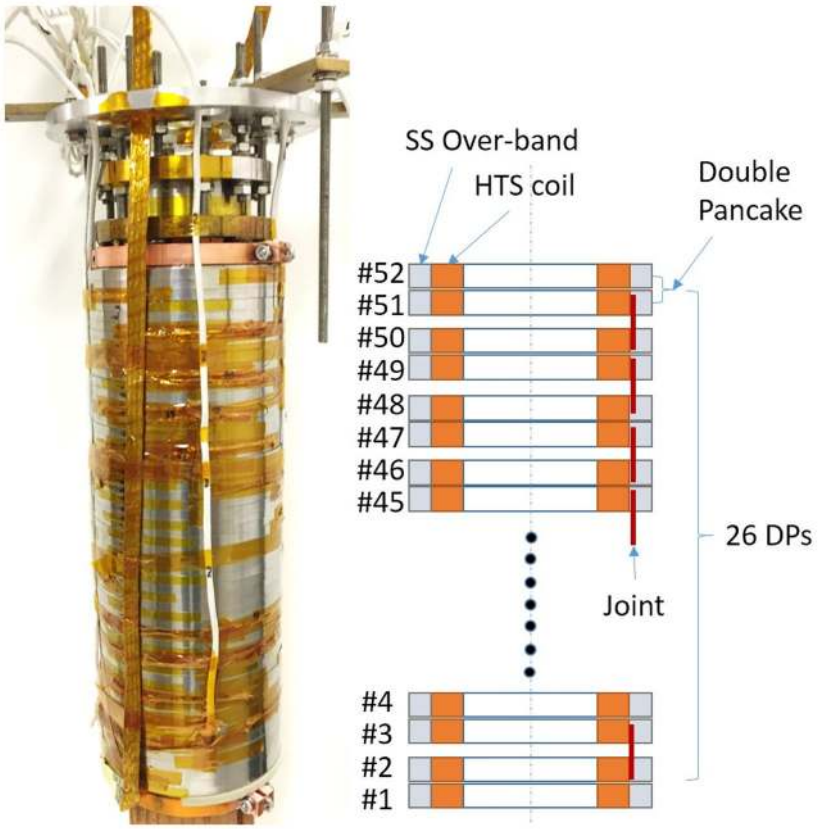

Fig. 1.
Photo and diagram showing double pancakes (DP) and overbanding layers in Coil 1.

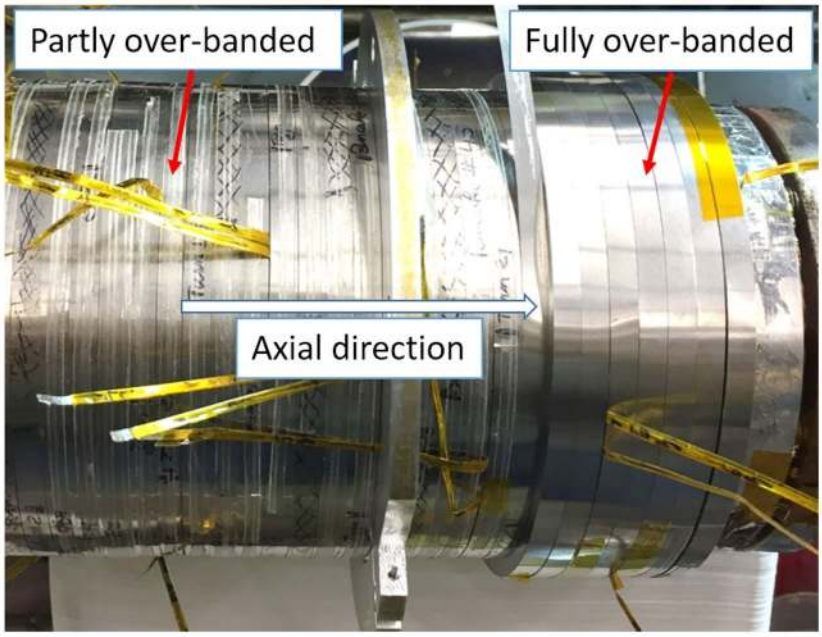

Fig. 2.
Photo for the overbanding process of Coil 1, the left side was partly overbanded with 21-layer SS tape, the right side was fully overbanded.

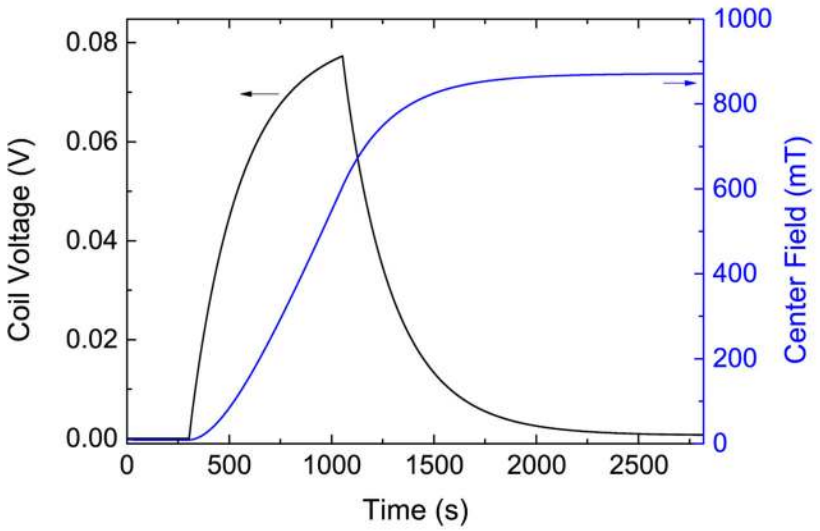

Fig. 3.
Coil voltage and center field evolution when Coil 1 was charged up from 0 A to 25 A.

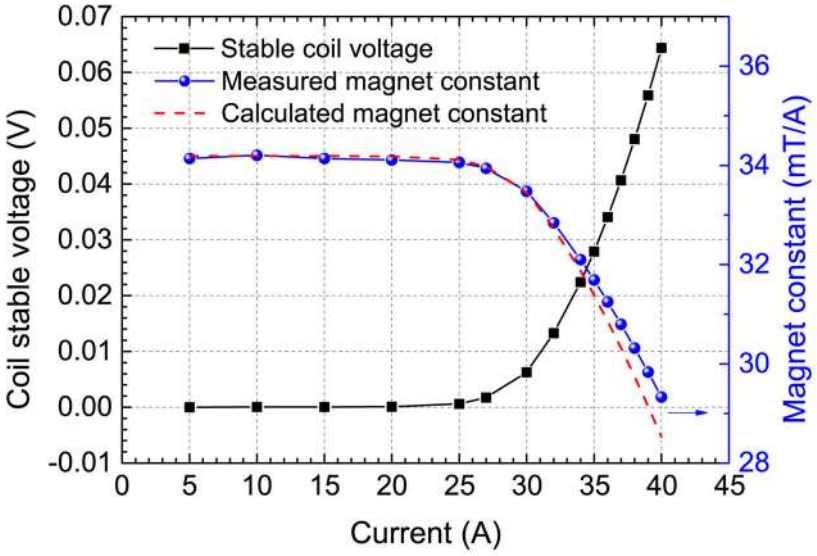

Fig. 4.

Coil voltage and magnet constant, center field divided by current, measured at different operation current at 77 K. The red dash line shows the calculated magnet constant according to the circuit model.

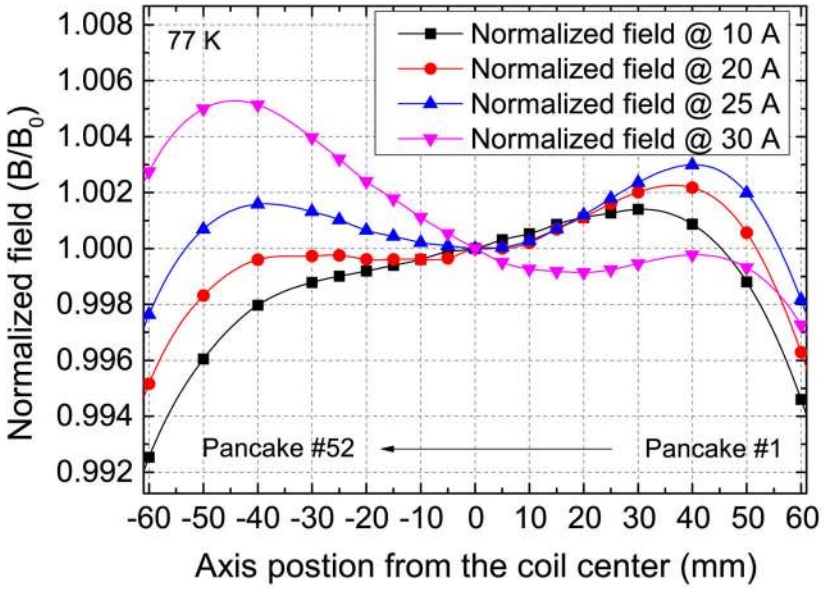

Fig. 5.

Normalized axial field (B/B_0) distribution at different operation current (I_{op}) at 77 K. The center field (B_0) values are 342.0 mT, 682.2 mT, 851.6 mT and 1004.3 mT for I_{op} =10 A, 20 A, 25 A, and 30 A, respectively.

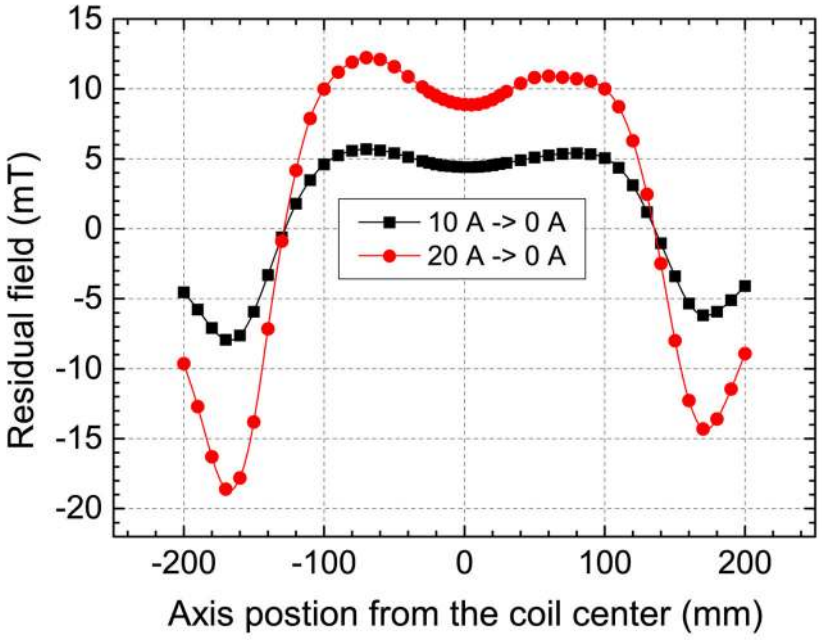

Fig. 6.

Screening-current-induced residual field distribution along the axis of Coil 1 after discharging from 10 A and 20 A.

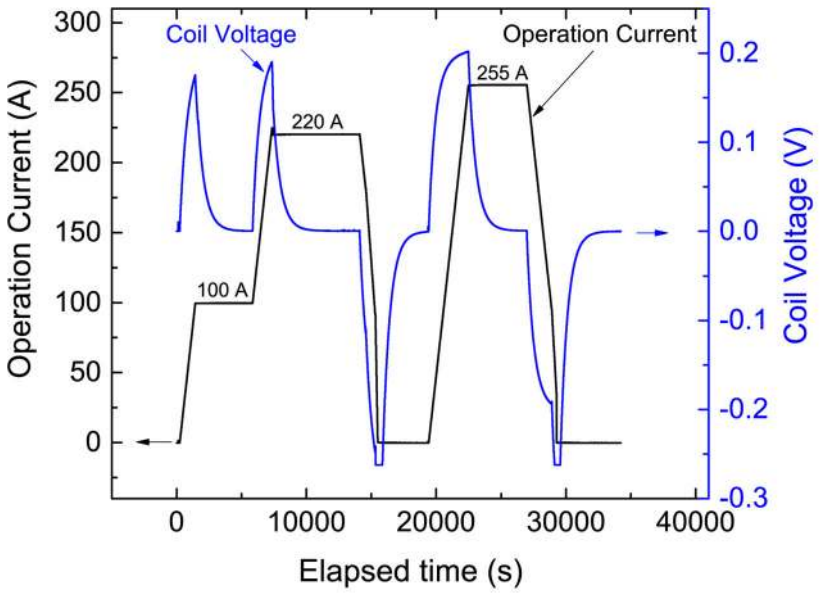

Fig. 7.
Operation current and coil voltage curves vs. elapsed time for the test at 4.2 K.

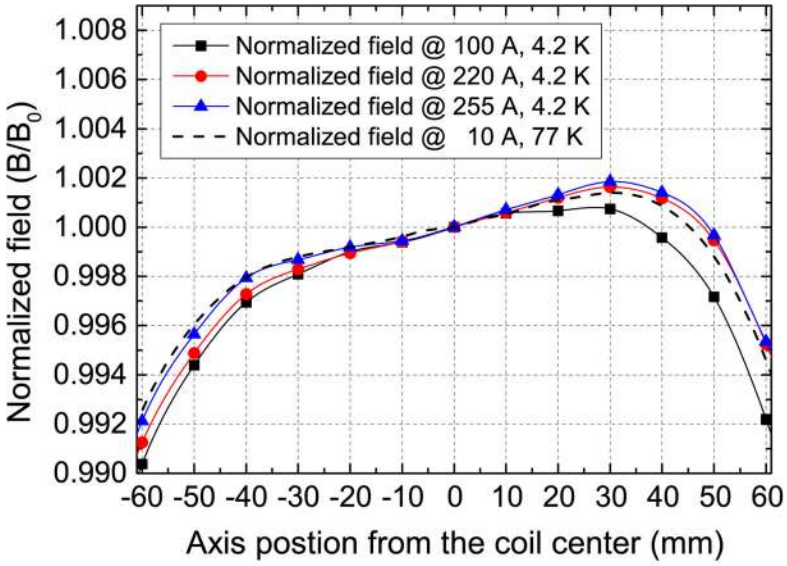

Fig. 8.

Normalized axial field (B/B_0) distribution of Coil 1 at different operation current (I_{op}) at 4.2K. The dash line shows the curve for I_{op} = 10A at 77 K. The center field (B_0) values are 3.42 T, 7.58 T and 8.78 T for I_{op} = 100 A, 220 A, and 255 A, respectively.

Table I

Properties and key design parameters for Coil 1.

Parameter	Unit	Coil 1
Field @ 4.2 K, 255 A	[T]	8.78
Critical Current @ 77 K (0.1 μV/cm)	[A]	35.7
Inductance (Computed)	[H]	2.43
Total # DP coils (notched)		26 (6)
# turns/pancake		185
# turns/notched pancake		177
REBCO length/DP	[m]	121.9
REBCO length/notched DP	[m]	116.7
Winding ID	[mm]	91.0
Winding ID (notched)	[mm]	92.35
OD without overband	[mm]	119.1
Overall height	[mm]	323.7
Overband thickness for 2×17 top/bottom pancakes	[mm]	6
Overband thickness for 18 center pancakes	[mm]	7

Table II

Table for L_m, τ and R_m values at 77 K.

Operation Current (A)	L_m/H	τ/s	R_m/mΩ
10	2.39	247	9.7
15	2.39	249	9.6
25	2.41	248	9.7

Table III

Table for L_m, τ, R_m and magnet constant values at 4.2 K.

Current/A	L_m/H	τ/s	R_m/mΩ	Magnet constant/(mT/A)
100	2.40	596	4.0	34.2
220	2.42	549	4.4	34.4
255	2.40	569	4.2	34.4